Available online at www.sciencedirect.com

ScienceDirect

Energy Procedia 148 (2018) 130–137

Energy Procedia

www.elsevier.com/locate/procedia

73rd Conference of the Italian Thermal Machines Engineering Association (ATI 2018), 12–14 September 2018, Pisa, Italy

Validation of an URANS approach for direct and indirect noise assessment in a high pressure turbine stage

Corrado Burberi[a*], Erika Ghignoni[a], Lorenzo Pinelli[a], Michele Marconcini[a]

[a]*Department of Industrial Engineering, Università degli Studi di Firenze, Via di Santa Marta 3, 50139 Firenze, Italy*

Abstract

In response to the continuous increase in aircraft noise pollution, computational aeroacoustic analyses are mandatory during the aero-engine design loop. In order to investigate the acoustic generation and propagation phenomena within a multi-stage turbomachinery, an experimental campaign on direct and indirect noise coming from a high pressure axial turbine stage has been carried out by *Politecnico di Milano* in the context of the European research project RECORD. The purpose of this work is to numerically predict both the direct noise produced by stator/rotor interactions and the indirect noise generated by the non-acoustic fluctuations coming from an annular combustor that impinge on the HPT stage by using URANS analyses. The computational results are in good agreement with experimental measures, confirming the possibility to include the numerical method during the engine design loop to assess noise emissions and suggest low noise design solutions.

Keywords: HP turbine; CFD; aeroacoustic; direct/indirect noise

1. Introduction

Given the exponential growth in civil air traffic and the continuous increase of new airport number during the last twenty years, global regulations on noise emission levels have become more and more stringent. As a result,

* Corresponding author: Tel.: +39-055-275-8795; Fax: +39-055-275-8755; E-mail address: corrado.burberi@tgroup.unifi.it

10.1016/j.egypro.2018.08.040

aeroacoustics has become one of the essential aspects in aeronautical engine design, and thus low noise criteria must be taken into account together with aerodynamic and aeromechanical requirements and constraints.

Commonly the engine noise is classified into broadband and tone noise. The broadband noise, mainly generated by turbulence and combustion, is quite difficult to be investigated experimentally due to its wide frequency spectrum. On the other hand, tone noise is composed of sound emissions at discrete frequencies and is commonly more annoying than broadband noise. Several internal noise sources contribute to the overall emission of an aircraft engine. Considering the reduction in fan and jet noise achieved in modern turbofan engines, turbine noise has now a relevant impact on the overall emission level. For the above reasons, in this study only turbine tone noise emissions have been numerically investigated.

The tone noise generated by turbines is due to two different contributes named direct and indirect noise. The direct noise emission is mainly caused by the unsteady interactions between adjacent blade rows. The indirect noise is generated by the interactions of non-acoustic unsteady disturbances coming from the combustor, which impinge on high pressure turbine stages. The acoustic waves produced by this interaction, propagate upstream and downstream within the turbo-machine up to the engine extremities decreasing or keeping constant their amplitude. In order to investigate the generation and propagation of acoustic waves in multi-stage turbomachineries, an experimental campaign dedicated to direct and indirect noise coming from a high pressure axial turbine stage has been carried out by *Politecnico di Milano* in the context of the European research project RECORD (*Research Core Noise Reduction*). In addition to aeroacoustics measurements, several computational analyses have been performed in order to evaluate the capability of different numerical method to correctly predict direct and indirect acoustic emissions. The aim of this study is to numerically evaluate the direct and indirect noise emissions of this high pressure axial turbine stage using an Unsteady RANS method and to validate this approach exploiting the acoustic measurement acquired during the project.

2. Test Case

The test-case consists of a full axial HPT stage which is representative of a first stage of present day aero-engine HPT. This facility is installed in a closed-loop test-rig of the *Politecnico di Milano*. Three different operating conditions have been investigated during the experimental campaign carried out in the context of the European research project RECORD. The numerical analyses presented and discussed hereafter are referred to the transonic operating point OP1 reported in Table 1.

The HPT stage consists of a stator row with 22 blades and a rotor row composed by 25 blades. The meridional channel has constant radius endwalls where the stage is installed and undergoes a widening just downstream rotor row (see Fig. 1). The air loop starts from a compressor composed by 16 blades and located outside the testing section to provide the required pressure condition. Then, passing through the discharge volute of compressor, the air reaches a centripetal Inlet Guide Vane with a honeycomb layer to obtain uniform flow on the HPT stage inlet. In order to acquire the acoustic emissions, the test-rig is instrumented with microphone arrays upstream and downstream the HPT stage. Concerning the indirect noise generation, eleven pulsating injectors with a frequency of 90 Hz have been used to reproduce a temperature fluctuation coming from a typical annular combustor. All the details on the stage configuration, blade design and noise measurements can be found in [1] and [2].

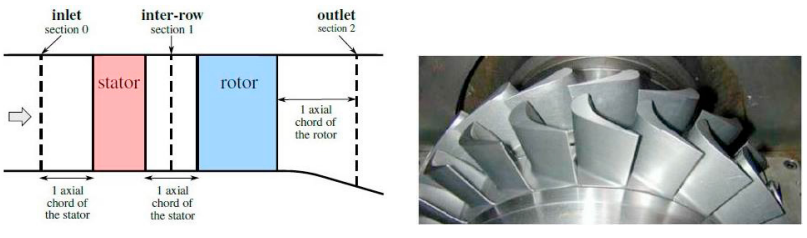

(a) (b)

Fig. 1. Meridional view (a) and full axial view (b) of the HPT stage.

OP1 conditions	
Expansion ratio	1.95
Inlet static temperature (K)	321.6
Inlet total pressure (Pa)	192000
Turbine rotational speed (rpm)	11100
Flow rate (kg/s)	6.05
Mach number	0.8
Reynolds number	6e+05

Table 1. Operating conditions.

3. Direct Noise

The direct tone noise emissions are mainly due to the unsteady interactions between adjacent blade rows in relative motion. The main causes of tone noise generation are rotor/stator interactions, vortex shedding, flutter and variation of blade unsteady load. These phenomena involve an interaction of circumferential non-uniformity in pressure field or turbulent-wake disturbances between rotating and stationary rows, which in turn, generates discrete tones at the blade passage frequency (BPF) and its higher harmonics. The acoustic waves produced by this interaction can be described as "spinning lobes" with a circumferential periodicity related to a scattering effect [3]. Once the acoustic waves have been generated, they can propagate upstream and downstream along turbo-machinery axis with two different behaviours: the *cut-off* acoustic waves are characterized by an exponential decrease of their amplitude whereas the *cut-on* waves keep a constant amplitude. These acoustic waves have a 3D shape which can be characterized by three coefficients: m (*circumferential order*) corresponds to the number of pressure lobes in circumferential direction; μ (*radial order*) describes the number of zero-crossing of pressure shape in radial direction; k_x (*axial wave number*) determinates the cut-on or cut-off nature of the wave propagation. Sound Power Level, commonly referred as Power Watt Level, has been used to compare numerical and experimental results. The PWL is a logarithmic value, which relates the power of an acoustic wave (W_a) obtained by integrating the acoustic intensity on a surface, to a reference power value (threshold of human hearing at 280 mm from the source). It is measured in dB and it is given by (1):

$$PWL = 10log_{10}\frac{W_a}{W_0} \tag{1}$$

3.1. Computational setup

Computational aeroacoustics (CAA) methods are derived from CFD unsteady methods as aeroacoustics problems, by definition, are time dependent phenomena and generally involve high frequency fluctuations. The main numerical methods currently in use for tone noise predictions of turbomachinery are [4]:

- Unsteady RANS (non-linear time domain method)
- Harmonic balance (non-linear multi-frequencies domain method)
- Time-linearized approaches (time-linearized single frequency domain method)

In this work, simulations were carried out with the TRAF code [5], a 3D URANS solver that uses a dual-time-stepping method to perform time accurate calculations. Given that acoustic fluctuations are purely unsteady phenomena, a non-linear time domain method allows an accurate computation of the rotor-stator interactions and at the same time the resolution of the acoustic generation and propagation phenomena. Once the computation reaches the time periodicity, a temporal DFT (Discrete Fourier Transform) algorithm is used to extract the harmonic content of the acoustic fluctuations. Then a circumferential DFT is applied to each time harmonic at a selected axial section to split the circumferential orders along the radius. Finally, each circumferential order is decomposed with a radial mode analysis in sheared and swirling flows in order to extract the single acoustic wave and to compute PWL values related to each acoustic traveling wave [6].

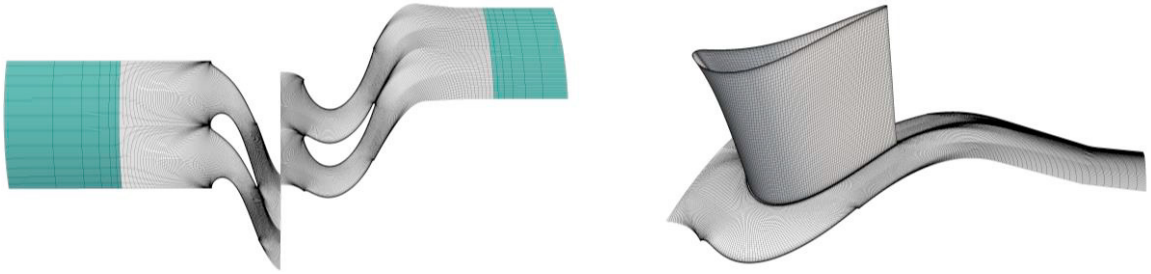

(a) (b)

Fig. 2. (a) Blade-to-blade view at midspan of H-grid with Buffer Zones (blue); (b) Full Navier-Stokes mesh (rotor blade).

The computational domain is discretized with a structured H-type grid consisting of 272×72×80 cells in the three coordinates direction *i*, *j*, *k* for the stator, and 260×72×80 cells for the rotor, for a total of about 3M cells. A visualization of the blade-to-blade mesh at midspan has been reported in Fig. 2(a), while the 3D mesh on the blade surface has been reported in Fig. 2(b). The inlet section has been placed 60 mm upstream the stator, corresponding to the axial position of the pulsating injectors, and the outlet section is 82.1 mm downstream from the rotor trailing edge. The outlet section cannot be placed at the microphone array location, as the noise acquisition system is quite far from the rotor trailing edge, and this would have required a huge computational domain and unnecessarily increased the computational cost, considering that cut-on waves under investigation does not change their amplitude during the axial propagation in a constant radius annular duct. The clearance areas at the stator hub and the rotor tip have not been meshed but the clearance effects have been included in the simulations by imposing a periodic boundary condition only on the hub and tip cells corresponding to the clearance height in span-wise direction [7]. The Wilcox k-ω turbulence model was used for turbulence closure. A full annulus approach with the real blade count (22/25) has been used for the unsteady analysis with a dual time stepping technique.

A steady state analysis, characterized by a single-vane approach with one-dimensional circumferentially averaged radial distribution of total pressure, total temperature and flow angles at the stage inlet was performed to verify the average working condition of the stage at the OP under investigations and to initialize the URANS analysis. The steady numerical results are in excellent agreement with the averaged experimental data, as can be seen in the comparisons shown in Fig. 3.

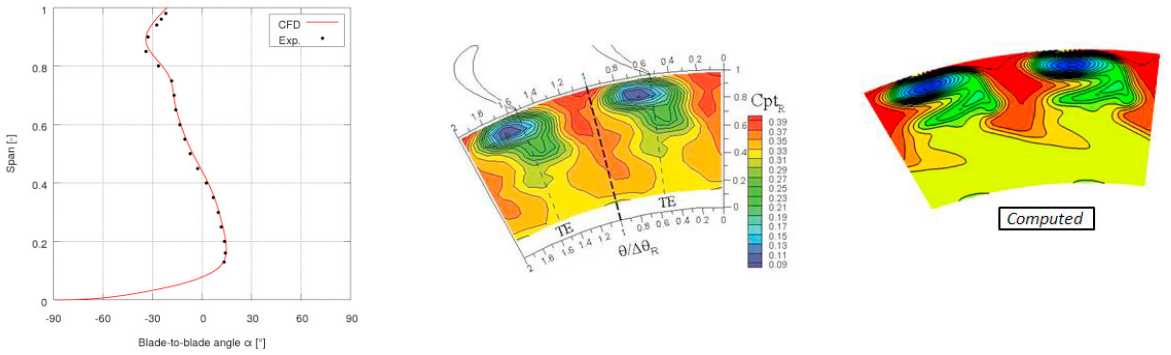

(a) (b)

Fig. 3. (a) Blade-to-blade flow angle and (b) relative total pressure coefficient at the rotor row outlet.

The first unsteady analyses have been dedicated to the prediction of direct noise emissions generated by the rotor-stator interaction, focusing on the acoustic wave with cut-on behavior at the 1×BPF (4625 Hz). Two radial modes ($\mu = 0$, $\mu = 1$) with circumferential order $m = +3$ are found responsible for the main acoustic emissions at the 1×BPF in according to the Tyler and Sofrin's rule [3].

A "buffer zone" technique is used in the URANS analysis to avoid numerical reflection at the domain inlet/outlet. This non-physical domain zones are added at the stage inlet/outlet and the computation boundary conditions are slightly modified to match experimental values at the extremities of actual domain (the interface between row grid and buffer zone mesh). This buffer zone, characterized by an axial grid stretching, acts as an adsorbing layer where physical outgoing wave are dumped due to the poor grid resolution so that the incoming spurious reflected disturbances at the domain inlet/outlet are low and further dumped by the grid stretching when traveling back in the buffer zone. With this technique, the amplitude of spurious reflection entering the physical domain is negligible compared to physical outgoing pressure wave. Several buffer zones with different cell number and stretching length have been tested to achieve an efficient damping effect. A lightweight inviscid endwall model has been used for the buffer zone sensitivity and quickly compare the effect of the different buffer zone parameters. The inviscid endwall mesh has been obtained reducing from 80 to 8 the cell number in span-wise direction *k* and removing endwall stretching. Cell number in the other direction is kept unchanged. Table 2 summarizes the test matrix of buffer zone configurations.

Buffer Zone type	Case α	Case β	Case γ	Case δ
Axial cell number	10	6	8	6
Length [mm]	100	50	50	75

Table 2. Buffer zone grid setup.

3.2. Tone noise results

An overall comparison between the numerical results of the different setup and the acoustic measurement for the 1×BPF emissions at the stator inlet and at the rotor outlet has been reported in Fig. 5 and 6 respectively. All four different buffer zone setups show a significant reduction of spurious reflected waves in terms of PWL. In particular, *case α* is characterized by the lowest values of spurious reflected waves at both domain sections. Anyway, comparing the total PWL values of reflected waves between *case α* and *case δ* at the inlet stage section and between *case α* and *case β* at the outlet stage section, the difference is quite low. Hence the use of *case α* buffer zone is not advisable since it increases unnecessarily the mesh dimension and consequently the computational cost. As a result, the *case δ* buffer zone setup has been selected for the domain inlet, while the *case β* buffer zone setup for the domain outlet.

Fig. 5 and 6 show a further significant result. Despite the use of a simplified grid model, the computed noise level is in good agreement with the experimental results. This results also confirms that the simplified discretization is capable to accurately evaluate the tone noise emissions for this HPT stage. 2D visualizations of the pressure fluctuation fields of the 1×BPF at the stator and rotor midspan with and without the use of buffer zone have been reported in Fig. 4. Without the buffer zone, the pressure wave fronts cannot cross the grid boundaries and so they are numerically reflected. However, with the buffer zone, the acoustic waves cross the physical domain boundaries without experiencing any decay, then they are dissipated within the buffer zone to avoid spurious reflection at the computational domain extremities where steady conditions are applied. For the acoustic post-processing, the buffer zone grids are removed (indeed they are not shown in Fig 4).

Fig. 4. Acoustic pressure perturbation at stator (left) and rotor (right) midspan section without and with buffer zone application.

The comparison between the tone noise emissions computed with a Full Navier-Stokes model and the experimental data is shown in Table 3. The computed total PWL of the outgoing pressure wave (downstream running for the outlet section, upstream running for the inlet section) is in a very good agreement with the experimental data. The slight discrepancies can be ascribed to the different axial positions of the noise acquisition system (see section 2) and to the presence of the structural asymmetric struts between the stage and microphones not included in the numerical studies. In all the computations, the spurious numerical reflections have been correctly damped by the buffer zones. The time evolution of acoustic waves at the 1×BPF at the outlet section in four equally spaced instants over a whole period (T), is shown in Fig. 7. The three rotating pressure lobes are clearly visible in this 2D visualization of acoustic perturbation and correspond to the acoustic wave with the circumferential order m = +3 which is the main responsible for the overall direct noise emission. The very good agreement between numerical and experimental results highlights the capability of URANS method to correctly predict direct tone noise emissions.

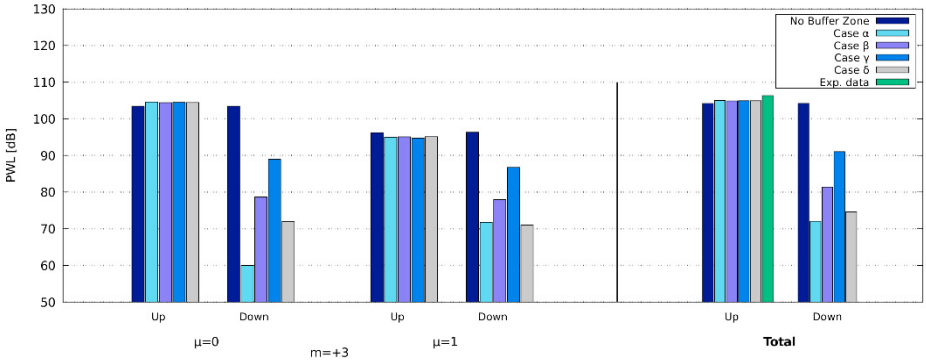

Fig. 5. 1×BPF: PWL for each radial orders and total values of downstream and upstream running waves at stator inlet.

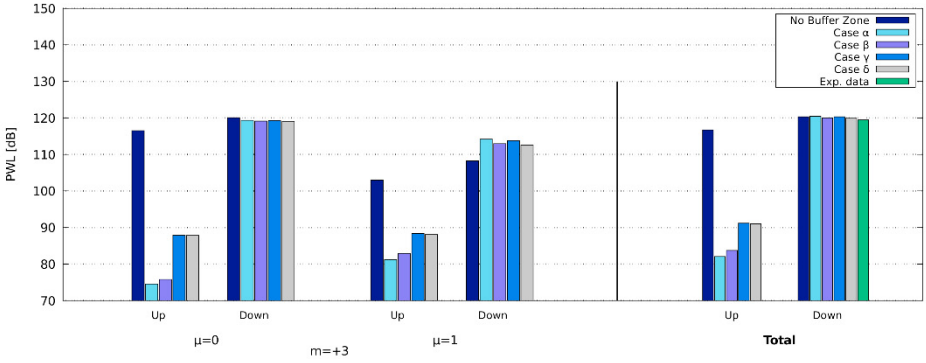

Fig. 6. 1×BPF: PWL for each radial orders and total values of downstream and upstream running waves at rotor outlet.

	PWL downstream running	PWL upstream running	Exp.data
Inlet section	83.4	105.0	106.3
Outlet section	121.4	102.9	119.5

Table 3. 1×BPF: total PWL values from Full Navier-Stokes computation at the stage inlet and outlet in comparison with experimental data.

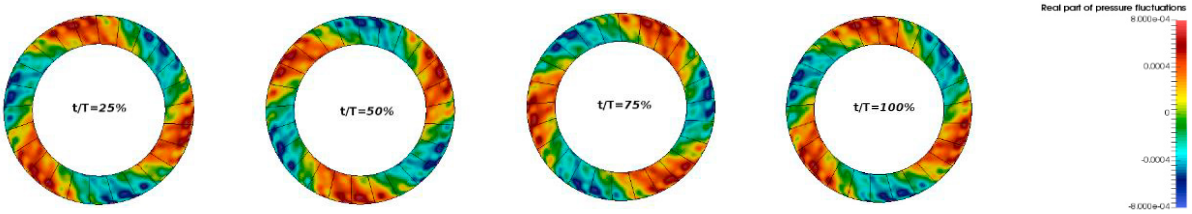

Fig. 7. 1×BPF: time evolution of instantaneous pressure at the rotor outlet. The overall fluctuation is dominated by circumferential order m = +3.

4. Indirect Noise

The indirect noise is generated when a fluid flow, characterized by a non-uniform entropy or vorticity distortion, is accelerated in or convected through turbine stages located downstream the combustion chamber. The non-acoustic time-varying fluctuation generates acoustic waves which propagate inside the turbine [8].

Again, an URANS analysis has been performed in order to assess the indirect acoustic emissions caused by a pulsating temperature disturbance (basically an entropy wave) coming from a typical combustor and convected downstream the HPT turbine stage under investigation. This analysis allows the estimation of the effects due to this fluctuation on the overall tone noise emitted by the HPT stage. The numerical analysis has been carried out using the same computational grid and numerical setup of the direct noise computation. The only difference concerns the inlet condition where a time-varying non-uniform 2D distribution of total temperature have been imposed to reproduce the temperature distortion coming from 11 tubular combustor chambers (one each two stator vanes as shown see Fig. 8 where two stator passages are reported). The computational two-dimensional inlet has been generated by superposing the values of total pressure and temperature fluctuations measured by FRAPPs (Fast-Response Aerodynamic Pressure Probes) to the circumferentially average quantities where the 11 injectors are located (four instants of the fluctuation are shown in Fig. 8).

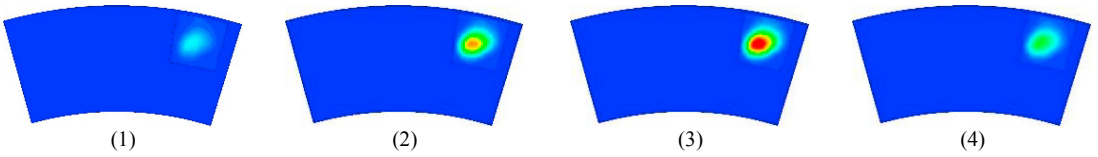

Fig. 8. Total temperature fluctuation at 4 equally-spaced time instants at stage inlet.

4.1. Indirect noise results

To shorten the computational time, a slight frequency correction has been applied to fluctuation frequency compared to the experiment: the pulsating frequency has been changed from 90.0 Hz to 92.5 Hz. In this way, two entire rotor revolutions occur during one injector pulsation as the rotational frequency of the stage at the operative point under investigation is equal to 185.0 Hz (11100 rpm). The eleven injectors are activated in phase and generate temperature spots (with the same velocity of the main flow in order to avoid further distortion). Such convected disturbances impinge on the HPT stage and generate the indirect tone noise characterized by a cut-on wave with m = 0 and μ = 0 (named *standing wave*) at the pulsating frequency (92.5 Hz). Furthermore, the overall 1×BPF emissions at the rotor outlet are now composed by a higher number of cut-on spinning waves. For this configuration, the Tyler and Sofrin's rule to define all the possible circumferential orders, becomes: $m = nB + kV + k'S$ where S is the number of the injectors. Accordingly, the principal additional cut-on modes are characterized by having m = -8 with μ = 0 and μ = 1 and m = +14 with μ = 0.

The comparison of the noise emissions in terms of PWL at the stage outlet (see Fig. 9) shows a good agreement between numerical results and experimental data. The additional cut-on waves at 1×BPF present a very low impact on the overall noise emissions. Indeed, the difference between total emissions with and without entropy waves is lower than 1 dB, for both computational results and measurements. The noise emissions of the cut-on wave at the 1×BPF (see left side Fig. 9) are differently redistributed as a results of incoming entropy wave. The comparison of indirect tone noise emission at the pulsating frequency (90 Hz, mode m = 0, μ = 0) has been reported the right side of Fig. 9.

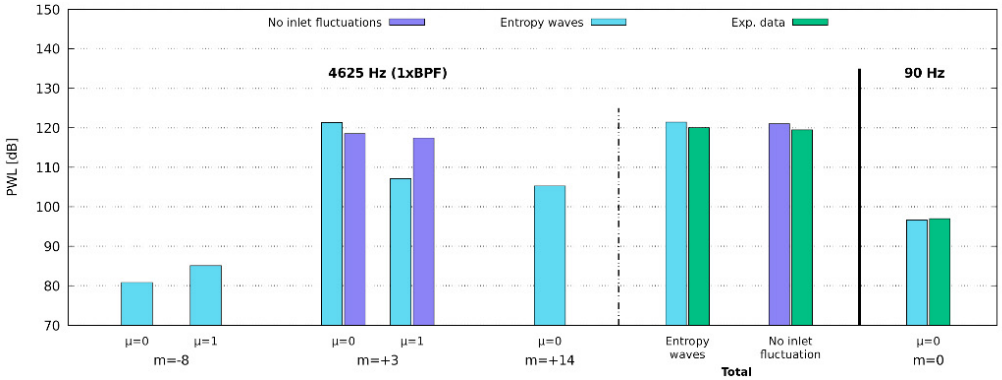

Fig. 9. 1×BPF (left): PWL for each radial orders and total values for two different cases; 0×BPF (right): PWL for circumferential order m = 0.

Globally, the numerical results show an excellent agreement with the measurement. It can be seen that the PWL value at the pulsating frequency (90 Hz) is low in comparison with the 1×BPF emission. Anyway, this contribution cannot be considered negligible in the overall noise emissions at the turbomachinery exhaust as the acoustic waves at this low frequency experience very low transmission losses when crossing the following turbine stages.

As a result, all these analyses, confirm the capability to correctly predict direct and indirect noise with URANS with dedicated numerical techniques as buffer zones. In summary, the inlet temperature fluctuation does not significantly modify the intensity of tone nose emission, but it increases the number of circumferential mode orders at 1×BPF and also generate additional cut-on waves (indirect noise) at the pulsating frequency (90 Hz) confirming the code capability to simulate indirect noise phenomena.

5. Conclusions

Over the last decades, the continuous expansion of the civil aviation field has led European countries to stimulate research programs with the aim at developing innovative techniques for aircraft noise reduction. Aeroacoustics has become one of the key aspects in aeronautical engine design, together with the aeroelasticity and aerodynamics. In this context, with the increase of available dedicated acoustic test campaign, also more and more accurate numerical models have been developed to assess the acoustic waves generation and propagation phenomena within aeronautical turbo-machineries. In the present study, full Navier-Stokes unsteady RANS have been performed to evaluate direct and indirect tone noise emissions of a high pressure transonic axial turbine stage. The investigated test case, installed in the closed-loop test-rig of *Politecnico di Milano* and used in the context of RECORD project, represents a first stage of present day aero-engine HPT. Firstly, steady state analyses have been performed to ensure satisfactory correspondence with the operating point under investigation in terms of average flow quantities. Then several analyses with a simplified domain model have been carried out to set-up the most efficient buffer zone setup to avoid spurious reflections. The buffer zones have been chosen as a compromise between damping of spurious reflected waves and the computational cost requirements. Finally, two full Navier-Stokes unsteady RANS were computed to predict the direct noise emissions, generated by the rotor/stator interaction in terms of PWL, and the indirect noise emissions, produced by a temperature pulsation at the stage inlet. The comparisons between numerical and experimental results show an excellent agreement for both direct and indirect noise emissions and a proper operation of buffer zones to damp the numerical reflections, thus validating the computational method. The direct noise emissions present a slight discrepancy probably due to the different positions of the noise extraction section. The inlet temperature fluctuation does not significantly modify the intensity of overall tone nose emission, but it increases the number of circumferential mode orders at 1×BPF; and more important, generates additional cut-on waves (indirect noise) at the pulsating frequency. In conclusion, the very good agreement between measurements and numerical results confirms the capability to correctly predict direct and indirect noise of turbine stages with an URANS method.

References

[1] V. Dossena, P. Gaetani, G. Persico and C. Osnaghi. “Investigation of the flow field in a high-pressure turbine stage for two stator-rotor axial gaps - part i: Three-dimensional time-averaged flow field.” *Journal of Turbomachinery*, 129(3) (2007): 572-579.

[2] K. Knobloch, L. Neuhaus, F. Bake, P. Gaetani, G. Persico “Experimental assessment of noise generation and transmission in a high-pressure transonic turbine stage.” *Journal of Turbomachinery*, 139(10) (2017): art. no. 101006.

[3] J.M.Tyler and T.G. Sofrin. “Axial flow compressor noise studies.” *Trans. Society of Automative Engineers 70*, (1962): 309-332.

[4] L. Pinelli, F. Poli, A. Arnone, S. Guérin, A. Holewa, J.R.F. Aparicio, R. Puente, D. Torzo, C. Favre, P. Gaetani, et al. “On the numerical evaluation of tone noise emissions generated by a turbine stage: an in-depth comparison among different computational methods.” In *ASME Turbo Expo 2015: Turbine Technical Conference and Exposition*, *American Society of Mechanical Engineers*, (2015).

[5] A. Arnone, M. Marconcini, A. Scotti Del Greco, E. Spano. “Numerical Investigation of Three-Dimensional Clocking Effects in a Low Pressure Turbine.” In *ASME Turbo Expo 2003*, (2003): GT2003-38414.

[6] L. Pinelli, F. Poli, E. Di Grazia, A. Arnone, F. Taddei, M. De Lucia, D. Torzo. “Numerical and Experimental study of the tone noise generation by a turbine rear frame.” *The 22nd International Congress of Sound and Vibration*, (2015).

[7] L. Cozzi, F. Rubechini, M. Marconcini, A. Arnone, P. Astrua, A Schneider, A. Siligardi. “Facing the challenge in CFD modelling of multistage axial compressor.” In *ASME Turbo Expo 2017*, (2017): GT2017-63240.

[8] K. Knobloch, A. Holewa, S. Guérin, Y. Mahmoudi, T. Hynes, F. Bake. “Noise transmission characteristics of a high pressure turbine stage.” *The 22nd AIAA/CEAS Aeroacoustics Conference, 2016*, (2016).